

NMR Detection of Protein ^{15}N Spins near Paramagnetic Lanthanide Ions

Michael John, Ah Young Park, Nicholas E. Dixon, and Gottfried Otting*

Australian National University, Research School of Chemistry, Canberra, ACT 0200, Australia

Received September 29, 2006; E-mail: gottfried.otting@anu.edu.au

The strong paramagnetism associated with lanthanide (Ln^{3+}) ions provides a unique source of structural information available for proteins that either have a natural lanthanide-binding site^{1,2} or are proteins site specifically tagged with an engineered lanthanide-binding group.^{3,4} It allows rapid 3D structure determinations of protein–protein and protein–ligand complexes,^{2,5} detailed structural studies near the lanthanide binding site,⁶ and the measurement of residual dipolar couplings.⁷ Among the paramagnetically induced NMR effects, pseudocontact shifts (PCS) of amide groups contain particularly useful structural information, because they report on the location of the nuclear (i.e., ^{15}N and $^1\text{H}^{\text{N}}$) spins with respect to the metal's magnetic susceptibility anisotropy ($\Delta\chi$) tensor anchored in the molecular frame.⁸

$$\Delta\delta^{\text{PCS}} = \frac{1}{12\pi r^3} \left[\Delta\chi_{\text{ax}} (3 \cos^2 \theta - 1) + \frac{3}{2} \Delta\chi_{\text{rh}} \sin^2 \theta \cos(2\phi) \right] \quad (1)$$

where $\Delta\chi_{\text{ax}}$ and $\Delta\chi_{\text{rh}}$ are the axial and rhombic components of the $\Delta\chi$ tensor, and (r, ϕ, θ) are the spherical coordinates of the nuclear spin in the tensor's principal axis system. Lanthanides like Tb^{3+} or Dy^{3+} generate large PCS that are measurable for nuclear spins as far as 40 Å from the metal ion.⁹

As a drawback, the strongest paramagnetic Ln^{3+} ions are invariably associated with pronounced paramagnetic relaxation enhancements (PRE). In particular, transverse PRE of ^1H spins render amide groups within about 15 Å of a Dy^{3+} ion and, hence, the entire metal binding site unobservable in ^{15}N -HSQC spectra. For most lanthanides, transverse PRE are dominated by the Curie mechanism⁸ and, therefore, can be approximated by

$$\Delta R_2^{\text{PRE}} = \frac{1}{5\pi r^6} \chi_{\text{iso}}^2 \gamma^2 B_0^2 \tau_{\text{R}} \quad (2)$$

where χ_{iso} is the metal's isotropic magnetic susceptibility, γ is the gyromagnetic ratio of the nuclear spin, B_0 is the magnetic field strength, and τ_{R} is the molecular rotational correlation time. Because of the strong dependence of PRE on the metal–nuclear distance r , additional spectra with much weaker paramagnetic ions such as Ce^{3+} have to be acquired to yield PCS information close to the metal center.

Alternatively, the scaling of PRE with γ^2 has been exploited in a range of protonless ^{13}C -detected experiments.¹⁰ ^{13}C spins are about 16-fold less sensitive to PRE effects than ^1H spins, so that the same PRE prevails 1.6-fold closer to the metal ion. Correspondingly, ^{15}N spins would be observable more than 2-fold closer.^{6,11} Much of this gain is, however, lost by the intrinsically lower sensitivity of these heteronuclear spins and the difficulty to assign broad resonances by correlation spectra with fairly long magnetization transfer periods.⁶

Here we present an approach that combines the advantage of ^1H detection with the favorable relaxation properties of ^{15}N and the resolution of the ^{15}N -HSQC spectrum to measure PCS for ^{15}N spins

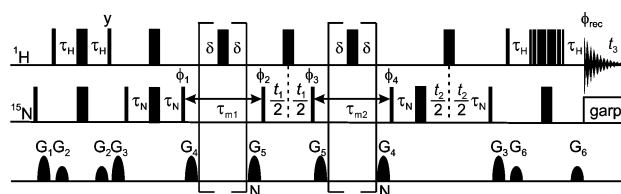


Figure 1. Out-and-back N_z -exchange experiment. Narrow and wide bars represent rf pulses with flip angles of 90° and 180° , respectively, applied with phase x unless otherwise indicated. The cycled phases were $\phi_1(y, -y)$, $\phi_2(x)$, $\phi_3(2x, 2(-x))$, $\phi_4(y)$, and $\phi_{\text{rec}}(x, 2(-x), x)$, and quadrature detection was achieved with States-TPPI applied to ϕ_2 and ϕ_4 . The delays τ_{H} , τ_{N} , and δ were set to 2.5, 2.75, and 1.5 ms, respectively. N was set to 160 using a MLEV-16 cycle for the ^1H pulses, resulting in mixing times ($\tau_{\text{m}1} = \tau_{\text{m}2}$) of 486 ms. The pulsed field gradients were applied along z with strengths (G_i) of 23.2, 8.7, 11.6, 14.5, 20.3, and 11.6 G/cm, and water suppression was achieved using the 3–9–19 sequence. Although the scheme was formally designed for water flip-back, the water resonance becomes saturated for long mixing periods. Omission of the ^1H pulses during τ_{m} resulted in a 20% increase of R_1 relaxation rates.

as close as 6 Å from the Dy^{3+} ion in a 30 kDa protein complex. The experiment relies on the chemical exchange of metal ions in a sample prepared with a mixture of diamagnetic and paramagnetic metals, and is implemented as an out-and-back experiment, where magnetization is stored as PRE-insensitive, longitudinal ^{15}N magnetization during two mixing times (Figure 1).

The use of two rather than one N_z mixing period distinguishes the experiment from conventional heteronuclear (N_z) exchange spectroscopy.^{12,13} This allows the generation of cross-peaks by a pathway (see Supporting Information) where magnetization is transferred from the diamagnetic to the paramagnetic state during $\tau_{\text{m}1}$, frequency-labeled during t_1 , and transferred back to the diamagnetic state during $\tau_{\text{m}2}$, avoiding the presence of transverse magnetization in the paramagnetic state at any other time than t_1 . Consequently, the observability of ^{15}N spins is limited by ^{15}N PRE rather than ^1H PRE.

The fraction of N_z magnetization transferred to the paramagnetic state during $\tau_{\text{m}1}$ and back during $\tau_{\text{m}2}$ is given by

$$M(\tau_{\text{m}})/M_{\text{tot}} = f_{\text{d}}^2 f_{\text{p}} (1 - e^{-k_{\text{ex}}\tau_{\text{m}}})^2 e^{-2R_1\tau_{\text{m}}} \quad (3)$$

where M_{tot} denotes the total N_z magnetization at the start of $\tau_{\text{m}1}$, f_{d} and f_{p} are the molar fractions of diamagnetic and paramagnetic protein, respectively, k_{ex} is the rate of metal exchange, R_1 is the longitudinal ^{15}N relaxation rate (assumed to be the same in both states), and it is assumed that $\tau_{\text{m}} = \tau_{\text{m}1} = \tau_{\text{m}2}$. To minimize losses, the experiment requires that k_{ex} is not much slower than R_1 .

We applied the experiment to the N-terminal domain of the exonuclease subunit ϵ of *E. coli* DNA polymerase III ($\epsilon 186$) in complex with the subunit θ . The active site of $\epsilon 186$ binds two divalent ions¹⁴ that can be replaced by a single Ln^{3+} ion.¹⁵ Although Ln^{3+} binding is quite tight with dissociation constants in the low μM range ($k_{\text{ex}} < 1 \text{ s}^{-1}$), catalysis of metal exchange by excess metal¹⁵ allows tuning of k_{ex} to values that compete with R_1 while

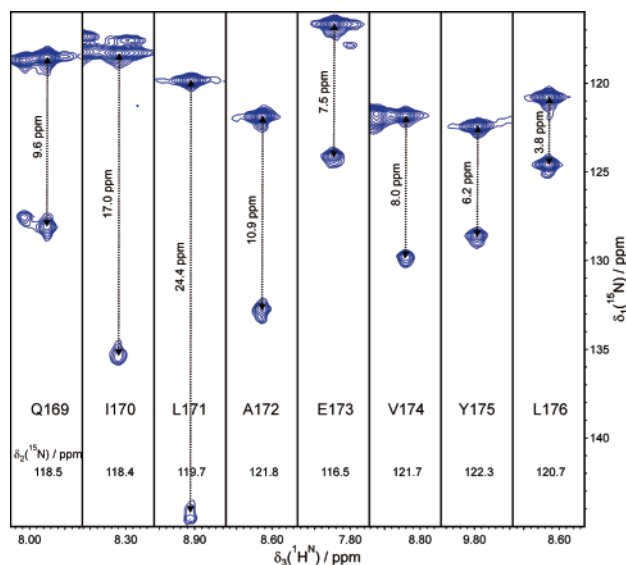


Figure 2. Selected strips from the 3D out-and-back N_2 -exchange spectrum of the 30 kDa $\epsilon 186/\theta$ complex, containing $^2H/^{15}N$ -labeled $\epsilon 186$. Parameters used: 25 °C, 0.8 mM $\epsilon 186/\theta$, equimolar ratio of Dy^{3+} and La^{3+} , 20 mM Tris (pH 7.2), 100 mM NaCl, Bruker Avance 800 MHz NMR spectrometer with TCI cryoprobe, $\tau_{m1} = \tau_{m2} = 486$ ms, $96 \times 64 \times 1280$ complex points, spectral widths of 32 ppm (^{15}N) and 20 ppm (1H), total experiment time 40 h. The strips are centered on the ^{15}N (F_2) and 1H (F_3) frequencies of the diamagnetic peaks of residues 169–176. Lines connect diagonal and exchange peaks and are labeled with the chemical shift difference which corresponds to the ^{15}N PCS.

avoiding excessive line-broadening because of the exchange or unspecific binding of lanthanide ions. By stepwise addition of a 1:1 mixture of Dy^{3+} and La^{3+} to $\epsilon 186/\theta$ we adjusted k_{ex} to about 5 s^{-1} , that is, 10-fold larger than R_1 . Under these conditions, about 35% of initial diamagnetic N_2 magnetization can be transferred to the paramagnetic state (and vice versa) during a single mixing period of 0.5 s, whereas 40% are retained in the diamagnetic state, and 25% are lost owing to R_1 relaxation. This presents a substantial gain over an experiment that starts from ^{15}N polarization (see Supporting Information).

Figure 2 shows strips from the 3D out-and-back N_2 -exchange spectrum for the helical segment from Q169 to L176. Each strip contains diagonal ($F_1 = F_2$) and exchange peaks (where F_1 reports the ^{15}N frequency of the paramagnetic state). The frequency difference between both peaks corresponds to the ^{15}N PCS. PCS values of up to 40 ppm and ^{15}N line widths of up to 130 Hz were measured for the $\epsilon 186/\theta/Dy^{3+}$ complex for a total of 156 residues of $\epsilon 186$. Notably, 61 of these could not be observed in the ^{15}N -HSQC spectrum of the pure $\epsilon 186/\theta/Dy^{3+}$ complex owing to excessive 1H PRE. For all remaining residues of $\epsilon 186$, for which the resonance assignments are known in the diamagnetic $\epsilon 186/\theta/La^{3+}$ complex, the ^{15}N - Ln^{3+} distances are shorter than 6 Å, diagonal and exchange peaks are overlapped, or the peaks are already weak in the diamagnetic ^{15}N -HSQC spectrum.

The spectrum also contains the expected diagonal and exchange peaks that are detected on the paramagnetic 1H resonance for residues with $r > 15$ Å. In the projection along F_2 , the four peaks form a rectangle and are therefore easy to identify.

For many of the residues close to the metal ion, the ^{15}N PCS values measured in the $\epsilon 186/\theta/Dy^{3+}$ complex were found to deviate substantially from values back-calculated using previously determined $\Delta\chi$ tensors of $\epsilon 186/\theta/Dy^{3+}$.¹⁶ This may be due to chemical exchange between multiple Ln^{3+} binding sites (up to three different,

closely spaced Ln^{3+} sites were observed in crystals of $\epsilon 186$ soaked with Dy^{3+} , ref 17) or due to structural differences between $\epsilon 186$ in the single crystal¹⁴ and the $\epsilon 186/\theta$ complex in solution. Notably, corresponding deviations in ^{15}N PCS values were also observed for the $\epsilon 186/\theta/Ce^{3+}$ complex. This indicates that the deviations report on structural rather than electronic features (see Supporting Information).

Ln^{3+} exchange rates on the time scale of the out-and-back N_2 -exchange experiment have also been observed for lanthanide-binding peptide tags⁴ (Su, X.C., personal communication). This makes the new experiment widely applicable for the assignment of ^{15}N resonances and measurement of ^{15}N PCS of proteins labeled with paramagnetic lanthanides.

Acknowledgment. We thank Nicolas D. Burns for help with the spectral analysis. M.J. thanks the Humboldt Foundation for a Feodor-Lynen fellowship. Financial support from the Australian Research Council for the Federation Fellowship for G.O. and the 800 MHz NMR spectrometer at ANU is gratefully acknowledged.

Supporting Information Available: Scheme of magnetization transfer pathways, comparison with an experiment starting from ^{15}N magnetization, correlation of deviations between experimental and back-calculated ^{15}N PCS for Ce^{3+} versus Dy^{3+} , $\Delta\chi$ tensor parameters, and a table of 1H and ^{15}N chemical shifts of $\epsilon 186$ in complex with θ and La^{3+} , Dy^{3+} or Ce^{3+} . This material is available free of charge via the Internet at <http://pubs.acs.org>.

References

- (1) (a) Bentrop, D.; Bertini, I.; Cremonini, M. A.; Forsen, S.; Luchinat, C.; Malmendal, A. *Biochemistry* **1997**, *36*, 11605–11618. (b) Biekovsky, R. R.; Muskett, F. W.; Schmidt, J. M.; Martin, S. R.; Browne, J. P.; Bayley, P. M.; Feeney, J. *FEBS Lett.* **1999**, *460*, 519–526. (c) Contreras, M. A.; Ubach, J.; Millet, O.; Rizo, R.; Pons, M. *J. Am. Chem. Soc.* **1999**, *121*, 8947–8948. (d) Ma, C.; Opella, S. J. *J. Magn. Reson.* **2000**, *146*, 381–384.
- (2) Pintacuda, G.; Park, A. Y.; Keniry, M. A.; Dixon, N. E.; Otting, G. *J. Am. Chem. Soc.* **2006**, *128*, 3696–3702.
- (3) (a) Feeney, J.; Birdsall, B.; Bradbury, A. F.; Biekovsky, R. R.; Bayley, P. M. *J. Biomol. NMR* **2001**, *21*, 41–48. (b) Wöhnert, J.; Franz, K. J.; Nitz, M.; Imperiali, B.; Schwalbe, H. *J. Am. Chem. Soc.* **2003**, *125*, 13338–13339. (c) Ikegami, T.; Verdier, L.; Sakhaei, P.; Grimme, S.; Pescatore, B.; Saxena, K.; Fiebig, K. M.; Griesinger, C. *J. Biomol. NMR* **2004**, *29*, 339–349. (d) Pintacuda, G.; Moshref, A.; Leonchik, A.; Sharipo, A.; Otting, G. *J. Biomol. NMR* **2004**, *29*, 351–361. (e) Prudencio, M.; Rohovec, J.; Peters, J. A.; Tocheva, E.; Boulanger, M. J.; Murphy, M. E. P.; Hupkes, H.-J.; Kosters, W.; Impagliazzo, A.; Ubbink, M. *Chem.—Eur. J.* **2004**, *10*, 3252–3260.
- (4) Su, X. C.; Huber, T.; Dixon, N. E.; Otting, G. *ChemBioChem* **2006**, *7*, 1599–1604.
- (5) John, M.; Pintacuda, G.; Park, A. Y.; Dixon, N. E.; Otting, G. *J. Am. Chem. Soc.* **2006**, *128*, 12910–12916.
- (6) Balayssac, S.; Jimenez, B.; Piccioli, M. *J. Biomol. NMR* **2006**, *34*, 63–73.
- (7) Tolman, J. R.; Flanagan, J.; Kennedy, M. A.; Prestegard, J. H. *Proc. Natl. Acad. Sci. U.S.A.* **1995**, *92*, 9279–9283.
- (8) Bertini, L.; Luchinat, C.; Parigi, G. *Prog. NMR Spectrosc.* **2002**, *40*, 249–273.
- (9) Allegrozzi, M.; Bertini, I.; Janik, M. B. L.; Lee, Y.-M.; Liu, G.; Luchinat, C. *J. Am. Chem. Soc.* **2000**, *122*, 4154–4161.
- (10) Bernel, W.; Bertini, I.; Felli, I. C.; Piccioli, M.; Pierattelli, R. *Prog. NMR Spectrosc.* **2006**, *48*, 25–45.
- (11) (a) Sadek, M.; Brownlee, R. T. C. *J. Magn. Reson., Ser. B* **1995**, *109*, 70–75. (b) Xia, B.; Wilkens, S. J.; Westler, W. M.; Markley, J. L. *J. Am. Chem. Soc.* **1998**, *120*, 4893–4894.
- (12) Farrow, N. A.; Zhang, O.; Forman-Kay, J.; Kay, L. *J. Biomol. NMR* **1994**, *4*, 727–734.
- (13) John, M.; Headlam, M.; Dixon, N. E.; Otting, G. *J. Biomol. NMR*, in press.
- (14) Hamdan, S.; Carr, P. D.; Brown, S. E.; Ollis, D. L.; Dixon, N. E. *Structure*, **2002**, *10*, 535–546.
- (15) Pintacuda, G.; Keniry, M. A.; Huber, T.; Park, A. Y.; Dixon, N. E.; Otting, G. *J. Am. Chem. Soc.* **2004**, *126*, 2963–2970.
- (16) Schmitz, C.; John, M.; Park, A. Y.; Dixon, N. E.; Otting, G.; Pintacuda, G.; Huber, T. *J. Biomol. NMR* **2006**, *35*, 79–87.
- (17) Park, A. Y. Ph.D. Thesis. Australian National University, Australia, 2006.

JA066950